DMD Fast Forward. Published on October 12, 2005 as doi:10.1124/dmd.105.004804

DMD #4804

APPLICATION OF A GENERIC PHYSIOLOGICALLY-BASED PHARMACOKINETIC MODEL TO THE ESTIMATION OF XENOBIOTIC LEVELS IN RAT PLASMA

F.A. Brightman, D.E. Leahy, G.E. Searle and S. Thomas

Cyprotex Discovery Ltd., 13-15 Beech Lane, Macclesfield, Cheshire, United Kingdom (F.A.B., D.E.L., G.E.S. and S.T.)

DMD Fast Forward. Published on October 12, 2005 as DOI: 10.1124/dmd.105.004804
This article has not been copyedited and formatted. The final version may differ from this version.

Running title: GENERIC PBPK MODEL APPLIED TO RAT PLASMA LEVEL ESTIMATION

Corresponding author: Dr. David E. Leahy

Address: Cyprotex Discovery Ltd., 13-15 Beech Lane, Macclesfield, Cheshire, United Kingdom, SK10 2DR

Telephone: +44 1625 505114

Fax: + 44 1625 505199

E-mail: d.leahy@cyprotex.com

Number of text pages: 37

Number of tables: 1

Number of figures: 10

Number of references: 40

Number of words in the Abstract: 247

Number of words in the Introduction: 723

Number of words in the Discussion: 1486

Non-standard abbreviations: ADME, absorption, distribution, metabolism and elimination; $AUC_{t1\text{-}tlast\text{-}DN}$, dose-normalized *AUC* from the first to the last recorded time points; CL_{int}, hepatic intrinsic metabolic clearance; DMPK, drug metabolism/pharmacokinetics; fu_p, fraction unbound in plasma; fu_pLin, linearized plasma protein binding parameter; fu_t, fraction unbound in the interstitial fluid; IQ, interquartile; $Kp_{IC:IFu}$, intracellular space/interstitial fluid (unbound) partition coefficient; MLFE, mean log fold error; PBPK, physiologically-based pharmacokinetic; PC, principal component; PD, pharmacodynamic(s); PK, pharmacokinetic(s); P_mS_m, permeability-surface area product for movement across the cell membrane; P_vS_v, permeability-surface area product for movement across the capillary wall; wMLFE, weighted MLFE.

ABSTRACT:

The routine assessment of xenobiotic *in vivo* kinetic behaviour is currently dependent upon data obtained through animal experimentation, although *in vitro* surrogates for determining key absorption, distribution, metabolism and elimination (ADME) properties are available. Here we present a unique, generic, physiologically-based pharmacokinetic (PBPK) model, and demonstrate its application to the estimation of rat plasma pharmacokinetics, following intravenous dosing, from *in vitro* data alone. The model was parameterized through an optimization process, employing a training set of *in vivo* data taken from the literature, and validated using a separate test set of *in vivo* discovery compound data. On average, the vertical divergence of the predicted plasma concentrations from the observed data, on a semi-log concentration-time plot, was approximately 0.5 log units. Around 70% of all the predicted values of a standardized measure of *AUC* were within threefold of the observed values, as were over 90% of the training set $t_{½}$ predictions and 60% of those for the test set; however, there was a tendency to over-predict $t_{½}$ for the test set compounds. The capability of the model to rank compounds according to a given criterion was also assessed: of the 25% of the test set compounds ranked by the model as having the largest values for *AUC*, 61% were correctly identified. These validation results lead us to conclude that the generic PBPK model is potentially a powerful and cost-effective tool for predicting the mammalian pharmacokinetics of a wide range of organic compounds, from readily-available *in vitro* inputs only.

DMD Fast Forward. Published on October 12, 2005 as DOI: 10.1124/dmd.105.004804
This article has not been copyedited and formatted. The final version may differ from this version.

Physiologically-based pharmacokinetic (PBPK) models are mathematical descriptions of the flow of blood throughout the body, developed for the simulation of xenobiotic absorption, distribution and elimination. The essential concepts were outlined over 60 years ago in a far-sighted paper (Teorell, 1937) that presented many of the mathematical relationships required to simulate blood flow and tissue distribution.

Simulation modelling ideas were developed further by Mapleson (Mapleson, 1973), in order to explain the effect of anaesthetics, and early attempts to apply the approach to drugs were published in the 1960's by Bellman et al. (Bellman et al., 1961). Probably the most important contributions in that period were made by Bischoff and Dedrick (Bischoff and Dedrick, 1968), who demonstrated that PBPK models could be used for the *a priori* prediction of the pharmacokinetics of thiopental. During the following decades, developments were made by academics such as Rowland (Rowland, 1986), Sugiyama (Sugiyama and Ito, 1998) and Amidon (Yu and Amidon, 1999), as well as scientists working in the environmental health field, in particular Anderson and Clewell (Andersen et al., 2002). Recent reviews (Grass and Sinko, 2002; Leahy, 2003) have discussed the application of these approaches to the prediction of pharmacokinetics in drug discovery.

It is of interest to us to apply the PBPK approach to the estimation of plasma levels in animals from *in vitro* data alone. If this can be achieved, with sufficient confidence in the outcome, a generic model for each species, including humans, could be used to address a wide range of problems where the estimation of pharmacological effects, safety margins and exposure limits is required. In particular, we believe that the exploitation of data from the growing number of validated *in vitro* toxicology assays requires a sound approach to the estimation of plasma and tissue levels within the whole animal. Since it is also our goal that predictive methods should be

DMD Fast Forward. Published on October 12, 2005 as DOI: 10.1124/dmd.105.004804
This article has not been copyedited and formatted. The final version may differ from this version.

applicable to a wide variety of chemicals prior to any animal experiment, we are interested in establishing generic PBPK models, which are parameterized for the physiology of the animal, independently of any specific xenobiotic. The properties of the xenobiotic that determine its overall kinetic properties could then be determined through the use of separate *in vitro* surrogates of the important absorption, distribution, metabolism and elimination (ADME) properties. Coupled with *in vitro* efficacy or toxicity data, simulation of the overall biological effect *in vivo* could become routine.

This paper describes the work we have done to parameterize a generic PBPK model for the rat, and to assess the reliability of the model in estimating plasma levels of xenobiotics, where these data are available from experimentation. To date, no other truly generic PBPK model has apparently been published, although there are numerous examples of compound-specific PBPK models for the rat, such as those for simulating the pharmacokinetics of tolbutamide (Sugita et al., 1982), diazepam (Igari et al., 1983), β-lactam antibiotics (Tsuji et al., 1983), cyclosporin (Bernareggi and Rowland, 1991) and a homologous series of barbiturates (Blakey et al., 1997). These and many other such models rely upon data derived from *in vivo* studies in order to estimate the extent of tissue distribution. Whilst computational models for predicting *in vivo* tissue/plasma partition coefficients from physicochemical and biochemical properties have been developed (Yokogawa et al., 1990; Poulin and Theil, 2000; Yokogawa et al., 2002; Rodgers, 2003), these are not generally applicable, being appropriate only for a particular class of basic compounds (Rodgers, 2003), for bases in general (Yokogawa et al., 1990; Yokogawa et al., 2002), or requiring modification of the fundamental model, depending upon distribution characteristics that cannot be established in advance with any certainty for novel compounds (Poulin and Theil, 2000). Furthermore, many of the published PBPK models for the rat also

utilize estimates of clearance determined *in vivo* (Tsuji et al., 1983; Bernareggi and Rowland, 1991; Blakey et al., 1997). The PBPK model presented herein predicts distribution and elimination kinetics in the rat from *in vitro* data alone, in a manner that is independent of ionization status and does not require *a priori* knowledge of *in vivo* pharmacokinetic properties.

In this paper, we have concentrated on predicting the *in vivo* pharmacokinetics of compounds for which plasma levels have been determined following an intravenous dose. Work that we have done to extend the model to predict plasma levels following an oral dose will be reported separately.

Methods

Model Inputs. A generic PBPK model, which enables prediction of the pharmacokinetic behaviour of any given compound dosed intravenously in a specified rat population, without recourse to data generated through *in vivo* studies, is described herein. The only compound-dependent inputs required by this model are:

- molecular weight;
- the octanol/water partition coefficient (*logP*);
- the octanol/water distribution coefficient at pH 7.4 ($logD_{7.4}$);
- all *pKa* values that affect the ionization status at pH 7.4;
- the hepatic intrinsic metabolic clearance (CL_{int});
- the fraction unbound in plasma (fu_p).

Model Description. The PBPK model is based upon that published by Bernareggi and Rowland (Bernareggi and Rowland, 1991), as shown in their Fig. 1, but with substantial modification of the tissue distribution (Fig. 1) and elimination (Fig. 2) components, and comprises a series of compartments representing 14 major organs and tissues in the body, interconnected by further compartments representing arterial and venous blood pools, according to the principles developed by Bischoff and others (Bischoff, 1975).

Administration of xenobiotics is via intravenous infusion, and their transport between the compartments that represent the organs and tissues occurs exclusively via blood flow.

Distribution into the organ and tissue compartments is 'diffusion limited' (Fig. 1). Thus, the cellular membrane represents a diffusion barrier, and movement between blood and tissue is modelled dynamically, rather than assuming that compound in the effluent blood of the tissue is in equilibrium with that within the tissue (Lutz et al., 1980), as in the 'flow-limited' PBPK model of Bernareggi and Rowland (Bernareggi and Rowland, 1991). The tissue is viewed as consisting of three, well-stirred sub-compartments (capillary bed, interstitial fluid and intracellular space), so that restricted diffusion across the capillary wall (for example, for modelling the blood-brain barrier) can also be represented. This arrangement is the minimum required to model adequately all possible restrictions to passive transport between blood and tissue. The possibility that movement across the plasma membrane is restricted to the unionized free compound is also accommodated in the model.

Elimination occurs from the compartment representing the liver, as in the model of Bernareggi and Rowland (Bernareggi and Rowland, 1991), but also from that representing the kidneys. Hepatic metabolism is modelled as a first-order process, the rate of which is determined by CL_{int} and the unbound compound concentration at the metabolic site. Renal excretion is represented by a physiologically-based model (Fig. 2) that has been developed from the work of Komiya et al. (Komiya, 1986; Komiya, 1987) and Katayama et al. (Katayama et al., 1990). According to this model, free compound within the plasma is filtered, within the glomerulus, into the lumen of the renal tubule, plus there may be additional active secretion of compound into the renal tubule lumen. Active renal secretion is characterized by an equation of the Michaelis-Menten form, where the maximum rate of tubular secretion and the Michaelis constant govern the rate of secretion of unbound compound into the tubular fluid. Both ionized and unionized species within the lumen of the renal tubule may be reabsorbed through solvent drag; however, only the

DMD Fast Forward. Published on October 12, 2005 as DOI: 10.1124/dmd.105.004804
This article has not been copyedited and formatted. The final version may differ from this version.

unionized fraction is subject to reabsorption through passive diffusion (Komiya, 1986). Inherent assumptions are that the permeability of the renal tubule to both water and solutes remains constant along its length (Komiya, 1986), and the renal tubule lumen and kidney tissue/capillary bed behave as well-stirred compartments, so that any compound reabsorbed from more distal portions of the tubule is made available for active secretion into the proximal tubule (consistent with the morphology of the nephron and its vasculature) (Katayama et al., 1990). Any compound within the renal tubule that escapes reabsorption is excreted unto the urine.

Model Parameters. The physiological parameters used in the model were obtained from the literature and are given in the Appendix (which is available online as supplemental data); these were scaled according to the actual body weights of the animals used in the *in vivo* studies being simulated. Tissue and organ volumes were derived from two comprehensive compilations of physiological data for use in pharmacokinetic models (ILSI, 1994; Brown et al., 1997), and represent the extravascular (combined interstitial fluid and intracellular space sub-compartments) volumes only. Blood flow rates for stomach, gut, pancreas, spleen and hepatic artery (and hence total liver blood flow) were obtained from a number of sources (Sasaki and Wagner, 1971; Malik et al., 1976; Nishiyama et al., 1976; Brown et al., 1997); all other blood flows were from Bernareggi and Rowland (Bernareggi and Rowland, 1991). The glomerular filtration rate and urine flow rate were taken from Davies and Morris (Davies and Morris, 1993), whilst the renal tubular lumen volume was derived from a textbook of physiology (Pitts, 1974). A haematocrit of 0.503 (Altman and Dittmer, 1971) was assumed.

Parameterization of the distribution and elimination components of the generic PBPK model for rat required the development of a number of correlation models. Two such models, for the prediction of parameters corresponding to the effective *in vivo* lipophilicity and plasma protein

binding, were derived through a process of optimization of the performance of the PBPK model, in terms of the estimation of experimental plasma levels. A comprehensive training set of *in vivo* data was used for this purpose. Both the optimization process and the training set data are described in greater detail below.

Instantaneous equilibration of the compounds between erythrocytes and plasma and between plasma and the interstitial fluid was assumed; i.e., there was no effective barrier to the transfer of compounds between the capillary bed and interstitial fluid model sub-compartments, and P_vS_v (Fig. 1) was set to a non-limiting value. The parameter P_mS_m (Fig. 1) was optimized across the training set and fixed at the same value for all compounds.

Intracellular space/interstitial fluid (unbound) partition coefficients ($Kp_{IC:IFu}$) were calculated for each compound using a model developed by Yokogawa et al. (Yokogawa et al., 1990; Yokogawa et al., 2002), which predicts tissue partition coefficients from a measure of lipophilicity and appropriate estimates of tissue lipid content. In this work, an estimate of the effective *in vivo* lipophilicity was used in the calculation, rather than a measure of actual lipophilicity (i.e. an experimental or calculated *logP*). Similarly, an estimate of the effective *in vivo* plasma protein binding was used as an input to the PBPK model, in place of a measured value for fu_p. The effective lipophilicity and fu_p for each training set compound were simultaneously determined through a grid search for the pair of values that generated the best estimate of experimental plasma levels. Regression analysis between the effective lipophilicity values for the training set compounds and the available input variables (listed above) showed that effective lipophilicities are best described as a simple linear combination of *logP* and the logarithm (to base 10) of the fraction unionized at pH 7.4. The best predictive model for the effective protein binding was found by linear regression, using a linearized protein binding parameter (fu_pLin) and the

DMD Fast Forward. Published on October 12, 2005 as DOI: 10.1124/dmd.105.004804
This article has not been copyedited and formatted. The final version may differ from this version.

logarithm of the fraction unionized at pH 7 to predict the logarithm of the effective fu_p values. The parameter fu_pLin is calculated from the *in vitro* fu_p as follows:

$$fu_pLin = log_{10}\left(\frac{1 - fu_p}{fu_p}\right)$$

An estimate of the blood cell/plasma partition coefficient was derived from a correlation between a set of measured blood cell/plasma partition coefficients and the variables *logP* and fu_pLin. This estimate was utilized along with the haematocrit and *in vitro* fu_p to calculate the blood/plasma concentration ratio (*R*).

The *in vitro* microsomal CL_{int}, scaled to ml/min/g liver, formed a direct input to the PBPK model as an estimate of the *in vivo* CL_{int}. Binding to albumin and lipoproteins also occurs in the interstitial fluid, and the fraction unbound in this sub-compartment (fu_t) was calculated from the effective *in vivo* fu_p, according to a methodology proposed by Poulin and Theil (Poulin and Theil, 2000). In order to simplify the model, specific binding to intracellular components was not considered.

The parameters describing passive reabsorption from the renal tubule (the permeability-surface area product) and reabsorption through solvent drag (the reflection coefficient) were calculated for each compound from *logP* and molecular weight, respectively. Although the PBPK model makes provision for representing active renal secretion, this capability was not used.

For the results presented here, stochastic simulations were performed in order to incorporate known variability in the animal body weights or imprecision in the values of the physicochemical parameters, microsomal CL_{int} and *in vitro* fu_p. For every set of input data (corresponding to

dosing of a single compound in a specified animal population), multiple iterations of the simulation were performed, with the values of the input parameters at each iteration being sampled randomly from the assumed distributions, these being either uniform or normal. Thus, variability was generated from the ranges or the means and standard deviations of the input data.

Training Dataset. The set of *in vivo* data employed in training the model comprised 214 instances of data (where an instance corresponds to a single plasma concentration-time profile) for 82 different compounds, and was derived from numerous published studies of intravenous dosing in rat. The compounds in this training set were drawn from many therapeutic areas and were selected for diversity in compound parameters. No attempt was made to avoid or eliminate compounds with non-linear pharmacokinetics or those subject to processes not explicitly modelled, such as active transport.

For the majority of the training set compounds, the required model inputs were determined at Cyprotex. Values for *logP*, $logD_{7.4}$ and *pKa* were obtained primarily using Sirius GLpKa apparatus (Sirius Analytical Instruments Ltd., UK), but in a small number of cases were generated using predictive software (ACD/PhysChem Batch, version 7.10, Advanced Chemistry Development, Inc., Toronto ON, Canada). Microsomal CL_{int} and fu_p were determined *in vitro* through incubation with hepatic microsomes and equilibrium dialysis, respectively. These data were supplemented by values from the literature where these were available.

Test Dataset. In order to objectively evaluate the performance of the model, an independent set of *in vivo* test data was constructed. This consisted of 194 instances of plasma concentration-time data for 134 discovery compounds dosed intravenously in rat. These data were supplied by several separate pharmaceutical/biotechnology companies, having been generated through their

internal pharmacokinetic studies, and the results presented here were derived in the absence of any prior knowledge of the *in vivo* pharmacokinetics or the chemical structures.

The test set compounds were varied in terms of physicochemical properties, and represented diverse therapeutic areas. Many of the requisite model inputs for these compounds were determined at Cyprotex, although the companies supplying the *in vivo* data also provided certain of the *in vitro* data, which were obtained through a variety of methods.

Calculation of the Plasma Concentration Weighted Mean Log Fold Error (wMLFE). For each pair of *in vivo* and simulated plasma concentration-time profiles, the log fold prediction error was determined at each simulated time point for which there were corresponding *in vivo* data, and the mean of these errors over all time points was calculated, to give an overall mean prediction ratio for each instance of simulated data. The wMLFE represents the weighted mean of these individual means. The weights used in the calculation arise from there being multiple instances and/or sources of *in vivo* data for several compounds, and hence the contribution of each individual log fold prediction error to the overall mean is weighted accordingly; i.e., so that each compound contributes equally, whatever the number of instances of *in vivo* data for that compound.

Principal Components Analysis. The values of seven variables for the training set compounds were transformed by subtracting the mean of the value, and dividing by the standard deviation, so that each transformed variable had a mean of zero and a standard deviation of one. The selected variables were: fractional charge at pH 7.4; fraction unionized at pH 7.4; $logD_{7.4}$; $logP$; $fu_{p}Lin$; $log_{10}(CL_{int})$ and $log_{10}(MW)$. Principal components analysis (Mardia et al., 1979) was performed on the transformed data, and the scores of the training set compounds recorded. The first three

principal components explained 81% of the variance of the dataset. The variable values for the test set were normalized in the same way, using the means and standard deviations of the values for the training set compounds. The scores of the test set compounds in the coordinates of the principal components of the training set were recorded.

Results

For any given set of input data, output from the PBPK model is in the form of a predicted plasma concentration-time profile. When stochastic simulations are performed for a single set of input data, each iteration generates a predicted profile, and hence the total output consists of a population of profiles that reflect the inherent uncertainty in the input data. Examples of typical simulation results, plotted on the same axes as the analogous *in vivo* data, are given in Fig. 3 for selected training set compounds and in Fig. 4 for a similar selection of test set compounds.

The simulated profiles in Figs. 3A and B and Figs. 4A and B illustrate accurate estimation of plasma concentrations over time, for selected training set and test set compounds, respectively. There is little variation within the population of profiles generated for either clozapine (Fig. 3A) or two example compounds from the test set (Figs. 4A and B), and the fit of the model output to the single set of observed data is almost exact in each case. In contrast, Fig. 3B demonstrates some observed *in vivo* variability, in this instance for erythromycin, and a combination of predicted variability and uncertainty, generated from both known variability in the animal weights and multiple estimates of *in vivo* fu_p and CL_{int}.

Some other simulation results are shown in Figs. 3C and D and Figs. 4C and D. The median predicted profile for pentazocine deviates from the observed profile, but the range of predicted profiles encompasses the *in vivo* data (Fig. 3C); hence, the model results can still be considered acceptable. Fig. 3D indicates somewhat inaccurate estimation of the *in vivo* tissue distribution of phenytoin, resulting in a tendency to under-predict plasma levels, although there is clearly a high degree of variability in the observed data for this compound, which is reflected in the model output. Fig. 4D shows a similar, but more pronounced overestimation of tissue distribution for an

example test set compound. However, the elimination half life has been accurately predicted for the test set compound represented in Fig. 4C.

For the remainder of the results presented here, the median of the population of predicted profiles generated from each set of input data was used as an individual estimate of the plasma concentration time course. In order to assess the overall performance of the model in terms of successfully predicting *in vivo* plasma levels, the plasma concentration wMLFE was determined for both the training and test sets; this statistic corresponds to the mean vertical deviation (in log units) of a simulated data point from a corresponding observed data point on a semi-log plot of plasma concentration versus time. The plasma concentration wMLFE values calculated for the training and test sets were 0.46 and 0.53, respectively, and hence the predicted plasma concentrations deviate from the observed values on average by around 0.5 log units. By way of illustration, the median predicted profiles shown in Fig. 3C and Fig. 4C both have an associated MLFE of approximately 0.5.

The frequency distributions of the actual mean fold errors in plasma concentration prediction for both sets of compounds are shown in Fig. 5A and B. A high proportion (72%) of plasma concentration predictions for the training set compounds are on average within a factor of five above or below the observed data points, and just a few (9%) are more than 20-fold in error overall (Fig. 5A). Whilst the majority (65%) of the predictions for the test set compounds are again within fivefold of the observed data on average (Fig 5B), the mean prediction error is less than twofold for a lower percentage of the test set compounds, and more than 20-fold for a greater proportion of these, compared to the training set.

DMD Fast Forward. Published on October 12, 2005 as DOI: 10.1124/dmd.105.004804
This article has not been copyedited and formatted. The final version may differ from this version.

The nature of the test set compounds for which plasma concentrations were poorly predicted by the PBPK model was explored in more detail by means of a descriptive classification model – developed using the RPART method of the R statistical software system (http://cran.us.r-project.org/doc/packages/rpart.pdf) – that provides some indication of biochemical and physicochemical commonalities between them (Fig. 6). Compounds demonstrating the characteristics of those that might be expected with a reasonably high degree of confidence to be poorly predicted, according to the classification model, were removed from the test set, including that for which the observed and predicted profiles are plotted in Fig. 4D. Thus, compounds with both $logD < 1.95$ and $fu_p \leq 0.065$ were eliminated; these criteria define a particular area of property space within which the likelihood of obtaining a poor plasma concentration prediction (mean fold error greater than 20) is approximately 60%, containing just 13% of the test set compounds overall, but 65% of those for which the predictions were in error, on average, by a factor of more than 20. Outside this area, the likelihood of a plasma concentration prediction being similarly poor is just 5%.

The frequency distribution of the plasma concentration mean fold prediction errors for the reduced test set (comprising 117 compounds) is shown in Fig. 5C. The error distribution pattern for this reduced set is somewhat different to that of the full set, with 73% of the predictions being within fivefold of the observed data, and a lower proportion being more than tenfold in error. The plasma concentration wMLFE for the reduced test set was 0.45, and therefore approximately the same as for the training set.

Although the primary outputs from the PBPK model are the predicted *in vivo* plasma concentration-time profiles that are generated, these can be utilized for estimation of standard pharmacokinetic (PK) parameters of interest, including area under the concentration-time curve

DMD Fast Forward. Published on October 12, 2005 as DOI: 10.1124/dmd.105.004804
This article has not been copyedited and formatted. The final version may differ from this version.

(*AUC*) and elimination half-life ($t_{½}$), allowing direct comparisons to be made with analogous *in vivo* data. Since different methods of extrapolating *AUC* from zero time to the first time point and from the last time point to infinity can vary in the estimates they yield, the simulation results were compared to observed data in terms of a standardized parameter, the dose-normalized *AUC* from the first to the last recorded time points ($AUC_{t1\text{-}tlast\text{-}DN}$), as well as $t_{½}$.

The capability of the PBPK model to accurately predict the selected PK parameters in rat has been evaluated in terms of the median values and inter-quartile (IQ) ranges of the predicted/observed ratios, for both the training and test sets, as given in Table 1. The respective summary data indicate that the prediction of both $AUC_{t1\text{-}tlast\text{-}DN}$ and $t_{½}$ for the training set compounds is generally successful. The median predicted/observed ratio is close to 1.0 for both parameters, and half of the predictions are on average within a range of approximately 0.5 to 1.5 times the observed values, although the statistics do indicate a slight tendency to under-predict $AUC_{t1\text{-}tlast\text{-}DN}$. The selected parameters are rather less accurately predicted for the test set compounds, as demonstrated by the greater deviation of the median predicted/observed ratios from a value of 1.0. Furthermore, the skew in the distribution of $AUC_{t1\text{-}tlast\text{-}DN}$ predictions is more apparent, whilst a notable over-prediction of $t_{½}$ for many of the compounds is also indicated.

The frequency distributions of the predicted/observed ratios of $AUC_{t1\text{-}tlast\text{-}DN}$ and $t_{½}$, for both the training and test sets, are more clearly demonstrated by the histograms shown in Figs. 7 and 8. The predicted/observed distributions for $AUC_{t1\text{-}tlast\text{-}DN}$ are similar for both sets of compounds, in both qualitative and quantitative terms (Fig. 7). Around half of all the predictions are within a factor of two above or below the observed values, and almost 70% are within a factor of three. The predicted/observed ratios conform closely to a normal distribution, although a slight tendency to under-predict $AUC_{t1\text{-}tlast\text{-}DN}$ is evident. Conversely, there is an obvious discrepancy

DMD Fast Forward. Published on October 12, 2005 as DOI: 10.1124/dmd.105.004804
This article has not been copyedited and formatted. The final version may differ from this version.

between the training set and test set predicted/observed distribution patterns for $t_{½}$ (Fig. 8). Estimation of this parameter for the training set is highly successful, with over 70% of the predictions being within twofold of the observed values, and more than 90% within threefold. Furthermore, the predicted/observed ratios are normally distributed. However, only 44% of the predicted test set $t_{½}$ values are within a factor of two of the observed values, although 60% are within a factor of three. There is also a clear bias towards over-prediction of this parameter, with a significant number of predictions being between two and five times the observed values, and a few even higher.

The performance of a predictive method, according to a given criterion, can also be represented graphically by means of a lift chart (Witten and Frank, 2000), such as that shown in Fig. 9. This plot illustrates the success rate of the PBPK model at selecting the 25% of the test set compounds with the largest values for $AUC_{\text{t1-tlast-DN}}$ (and therefore with the lowest plasma clearances). The horizontal axis shows the sample size as a percentage of the total number of compounds comprising the test set, whilst the vertical axis indicates the percentage of compounds correctly selected according to the stated criterion. The diagonal line represents the expected success rate if the selections were made at random, whilst the plot that would be generated by a 100% success rate is indicated by the line on the far left, which reaches a maximum (all selections correct) at a sample size equal to 25% of the total number of compounds. The actual performance of the PBPK model at ranking compounds according to $AUC_{\text{t1-tlast-DN}}$ is shown by the central line. The plot demonstrates that of the 25% of the test set compounds ranked by the PBPK model as having the largest values for $AUC_{\text{t1-tlast-DN}}$, 61% have been correctly identified. This is clearly substantially greater than the level of success to be expected (25%) if the compounds were selected at random.

DMD Fast Forward. Published on October 12, 2005 as DOI: 10.1124/dmd.105.004804
This article has not been copyedited and formatted. The final version may differ from this version.

In order to visualize the multivariate distributions of the training and test set compounds in the input space of the PBPK model, the scores for the first versus second and third versus second principal components were plotted for the training and test sets (Figs. 10A and B, respectively). It can be seen from Fig. 10B that the training set compounds fall into three reasonably well-separated groups. Furthermore, distinct physicochemical attributes can be ascribed to each of these groups. The compounds having their second principal component (PC) score less than zero (PC2 < 0) are strong bases, all having fractional charge at pH 7.4 of 0.56 or greater. The compounds with PC2 > 0 are acids and weaker bases, having fractional charge at pH 7.4 of 0.355 or less (see Fig. 10A and B). This set of compounds can be sub-divided on the value of the third PC. The group of 12 compounds with PC3 > 1 are all strong acids. The other compounds, with PC3 < 1, are bases or weaker acids, with a fractional charge at pH 7.4 greater than -0.545 (Fig. 10B). Thus, the three groups correspond to (i) strong bases, (ii) strong acids and (iii) weak/moderate acids and bases. The first PC is dominated by lipophilicity (*logP*, $logD_{7.4}$), plasma protein binding and intrinsic clearance, and displays a continuum of values for the training set (Fig. 10A).

The test compounds show some similarities, but also significant differences, to the training set scores. The first PC is again mostly a continuum, but with three outliers having PC1 > 4, compared to one for the training set. The distributions of the second and third PC values are, however, clearly different from those of the training set. The distributions for the test set are more continuous, so the separation into the three groups observed in the training set is not so clearly seen in the test set. Furthermore, whilst there are nascent clusters that correspond to those in the training set, the test set centres – particularly for groups (ii) and (iii) – are displaced relative to those of the training set.

Discussion

The PBPK model is potentially the most powerful tool currently available for: predicting *in vivo* PK; investigating the physiological and chemical interactions that give rise to organism- and compound-dependent PK, and linking with pharmacodynamics (PD) to provide an integrated PK/PD view of therapeutic and/or toxic effects of xenobiotics. However, the lack of a generic model that can be applied to a wide range of compounds, and/or can utilize inexpensively- and reliably-determined inputs for any given compound has, thus far, prevented widespread adoption of the PBPK modelling approach for PK prediction. We have developed a generic PBPK model for the rat that overcomes this obstacle, and thereby facilitates the routine and cost-effective prediction of PK. In principle, a similar model can be derived for any species for which the relevant physiological data are available; we have described an analogous model for the human in the accompanying paper (Brightman et al., 2005).

Recent developments in both the pharmaceutical industry and in those sectors of the manufacturing industry that produce environmental chemicals have increased the need for facile prediction of PK in man and other species. Within the pharmaceutical industry, the realization that consideration of pharmacokinetic and toxicity criteria during drug discovery will reduce the likelihood of costly failure during development has driven a greater requirement for PK data. Within the manufacturing industry, increasingly stringent international legislation concerning the safety of new and existing compounds necessitates quantification of the putative extent and duration of exposure in a variety of possible scenarios. At variance with the need to generate more PK data is the desire, both for cost and ethical reasons, to reduce animal experimentation where possible. The integration of *in vitro* ADME data and *in silico* methods can address this

dilemma, with PBPK modelling offering several advantages over alternative *in silico* or computational methods for the prediction of PK.

The first such advantage is that a PBPK model is likely to be more robust than alternative predictive methods. A large proportion of the variation in the pharmacokinetic behaviour of compounds can be explained by the physiological and biochemical processes involved in xenobiotic distribution, metabolism and elimination that are, at least partially, independent of the properties of the compounds. These processes are represented by the parameters and differential equations of the PBPK model. Thus, for example, the approach of *in vivo* plasma clearance to a maximal value with increasing hepatic elimination is determined by the limiting effect of hepatic blood flow. Similarly, whilst the partitioning of compounds from plasma into tissues is compound dependent, the relative extent of the distribution of lipophilic and hydrophilic compounds is dependent on the volumes of adipose and muscle tissue, respectively, whilst differences in their distribution rates are determined, in part, by the specific perfusion rates of these tissues. Many alternative approaches to predicting pharmacokinetic behaviour rely upon explaining all of the variation between compounds through a statistical model, with consequent dependence on the training data composition. Application of such methods can be expected to result in inaccurate predictions when applied to areas of chemistry outside of, or poorly represented within, the training data. As we have illustrated (Fig. 10), there are distinct differences in physicochemical and ADME-related properties between marketed drugs and compounds typical of those in drug discovery. Consequently, a statistical model that has been trained using data for existing drugs will most likely have a limited ability to generalize to typical discovery compounds. Within the generic PBPK model, the use of such models has been restricted to calculation of a small number of internal variables. In addition, these internal models

DMD Fast Forward. Published on October 12, 2005 as DOI: 10.1124/dmd.105.004804
This article has not been copyedited and formatted. The final version may differ from this version.

have been built using data from different, though overlapping, sets of compounds. These measures reduce the risk of poor prediction when the PBPK model is applied to novel areas of chemistry. The model validation results described herein demonstrate that the pharmacokinetic properties of the outlying test set compounds (see Fig. 10A) are well predicted, despite these compounds being outside the parameter space of the training set.

A second advantage is that the PBPK model predicts plasma concentration-time profiles, from which all required PK parameters can be calculated using standard formulae. By contrast, other approaches are usually restricted, in practice, to the prediction of one parameter. Consequently, if a number of parameters are to be considered in decision-making, corresponding models must be obtained for each. Assuming reliable models can be derived for the parameter space being studied, the individual parameters predicted by each model (for example, clearance, half-life and volume of distribution) must be consistent with each other in order to be of value in decision-making. A PBPK model predicts a consistent set of standard parameters for a given compound, calculated from a single predicted plasma profile. In addition, the simulated plasma or tissue profiles can be used as a basis for determining additional, non-standard parameters, such as the time following dosing for which the plasma or tissue concentration is greater than a specified value, which can be related to therapeutic and/or toxic thresholds and therefore used to estimate relevant exposure.

One possible role of the PBPK model in drug discovery is to enable drug metabolism/pharmacokinetics (DMPK) scientists to reliably identify those compounds that are likely to have suitable *in vivo* PK. The model provides two sets of data to this end: the predicted plasma and tissue concentration-time profiles, and PK parameters derived from the plasma profile. Either, or both, can be used in compound selection. If, for instance, the *in vivo* potency is

DMD Fast Forward. Published on October 12, 2005 as DOI: 10.1124/dmd.105.004804
This article has not been copyedited and formatted. The final version may differ from this version.

known or can be estimated, then the tissue or plasma profiles can be used to select compounds that have the longest durations at concentrations greater than that required for therapeutic effect. Alternatively, total exposure, as measured by dose-normalized *AUC*, may be used as a selection criterion.

The effectiveness of PK parameter prediction can be determined by relative accuracy and/or the ability to rank compounds successfully. Anecdotally, we have observed that drug discovery DMPK scientists would value tools enabling predictions to be made within a three- or sometimes twofold margin of error. We have shown that the PBPK model predicts $t_{½}$ and $AUC_{\text{t1-tlast-DN}}$ within threefold of the observed values for, respectively, 60% and almost 70% of a test set composed of discovery compounds. Assessment of the ranking capability of a predictive method can be performed by means of a lift chart, which can be used to quantitatively predict the likely consequences of making a particular operational decision. We have illustrated (see Fig. 9) an arbitrary scenario in which the identification of compounds with $AUC_{\text{t1-tlast-DN}}$ in the top quartile of the test set is required. Using the generic rat PBPK model to select the 25% of the test set with the highest $AUC_{\text{t1-tlast-DN}}$ results in 61% of the required compounds being selected, corresponding to an enrichment of more than 2.4-fold compared to random selection. In contrast, making the selection based on the 25% of compounds with the lowest intrinsic clearance results in 39% of the required compounds being selected, an enrichment of less than 1.6-fold (not shown). Specifying different selection criteria enables a series of curves to be generated, from which the potential benefits of the different strategies, in terms of the enrichment of compound selection, can be compared.

We have described our findings concerning the current version of a generic rat PBPK model, but model improvement is ongoing. As for statistical model development, additional compounds can

be added to the optimization training set, and additional descriptors assessed for their ability to predict the optimization parameters. However, a further advantage of the PBPK model is that its predictive capability can be improved by adding new features that represent additional physiological or biochemical processes, or by improving extant features of the model. The motivation can be to understand specific determinants of observed PK and/or to address shortcomings in the predictions. In the latter case, prioritization can be guided by identified weaknesses in the model. Thus, the observation that hydrophilicity coupled with high plasma protein binding is a strong indicator of poor plasma concentration prediction has guided us to improve the modelling of renal clearance. Additionally, we are developing a model of the blood-brain barrier, initially as a passive permeability barrier. These developments should lead to both significantly more accurate prediction of plasma PK, and more realistic prediction of the time course of compound concentration in the brain. Other factors such as non-linearity, specific transport processes and population effects, which are not explicitly described in the current model, could also be explored using the PBPK approach.

Developing the PBPK model for the rat has enabled us to verify that it is possible for such a model to generalize reliably outside the property space of the training set. However, the greater value to industry lies in being able to predict PK for human subjects exposed to xenobiotics. The work we have carried out in developing and validating a similar generic PBPK model for human is described in the accompanying paper (Brightman et al., 2005).

Acknowledgements

The authors thank Dr. Darwin Cheney, for his helpful comments on the manuscript.

References

Altman PL and Dittmer DS (1971) Blood physical properties, in *Biological Handbooks: Respiration and Circulation* (Altman PL and Dittmer DS eds), Federation of American Societies for Experimental Biology, Bethesda.

Andersen ME, Green T, Frederick CB and Bogdanffy MS (2002) Physiologically based pharmacokinetic (PBPK) models for nasal tissue dosimetry of organic esters: assessing the state-of-knowledge and risk assessment applications with methyl methacrylate and vinyl acetate. *Regul Toxicol Pharmacol* **36:**234-245.

Bellman RR, Jacques JA and Kalaba R (1961) Mathematical models in chemotherapy, in *Fourth Berkley Symposium on Mathematical Statistics and Probability* (Neyman J ed), pp 57-66.

Bernareggi A and Rowland M (1991) Physiologic modeling of cyclosporin kinetics in rat and man. *J Pharmacokinet Biopharm* **19:**21-50.

Bischoff K and Dedrick R (1968) Thiopental pharmacokinetics. *J Pharm Sci* **57:**1346-1351.

Bischoff KB (1975) Some fundamental considerations of the applications of pharmacokinetics to cancer chemotherapy. *Cancer Chemother Rep* **59:**777-793.

Blakey GE, Nestorov IA, Arundel PA, Aarons LJ and Rowland M (1997) Quantitative structure-pharmacokinetics relationships: I. Development of a whole-body physiologically based model to characterize changes in pharmacokinetics across a homologous series of barbiturates in the rat. *J Pharmacokinet Biopharm* **25:**277-312.

Brightman FA, Leahy DE, Searle GE and Thomas S (2005) Application of a generic physiologically-based pharmacokinetic model to the estimation of xenobiotic levels in human plasma. *Drug Metab Dispos* **in press**.

Brown RP, Delp MD, Lindstedt SL, Rhomberg LR and Beliles RP (1997) Physiological parameter values for physiologically based pharmacokinetic models. *Toxicol Ind Health* **13:**407-484.

Colburn WA and Gibaldi M (1977) Plasma protein binding and metabolic clearance of phenytoin in the rat. *J Pharmacol Exp Ther* **203:**500-506.

Davies B and Morris T (1993) Physiological parameters in laboratory animals and humans. *Pharm Res* **10:**1093-1095.

Grass GM and Sinko PJ (2002) Physiologically-based pharmacokinetic simulation modelling. *Adv Drug Deliv Rev* **54:**433-451.

Hanada E, Ohtani H, Kotaki H, Sawada Y and Iga T (1997) Determination of erythromycin concentrations in rat plasma and liver by high-performance liquid chromatography with amperometric detection. *J Chromatogr B Biomed Sci Appl* **692:**478-482.

Ichimura F, Yokogawa K, Yamana T, Tsuji A and Mizukami Y (1983) Physiological pharmacokinetic model for pentazocine. I. Tissue distribution and elimination in the rat. *Int J Pharm* **15:**321-333.

Igari Y, Sugiyama Y, Sawada Y, Iga T and Hanano M (1983) Prediction of diazepam disposition in the rat and man by a physiologically based pharmacokinetic model. *J Pharmacokinet Biopharm* **11:**577 - 593.

ILSI (1994) Physiological Parameter Values for PBPK Models, International Life Sciences Institute (ILSI) Risk Science Institute (RSI).

Katayama K, Ohtani H, Kawabe T, Mizuno H, Endoh M, Kakemi M and Koizumi T (1990) Kinetic studies on drug disposition in rabbits. I. Renal excretion of iodopyracet and sulfamethizole. *J Pharmacobiodyn* **13:**97-107.

Komiya I (1986) Urine flow dependence of renal clearance and interrelation of renal reabsorption and physicochemical properties of drugs. *Drug Metab Dispos* **14:**239-245.

Komiya I (1987) Urine flow-dependence and interspecies variation of the renal reabsorption of sulfanilamide. *J Pharmacobiodyn* **10:**1-7.

Leahy DE (2003) Progress in simulation modelling for pharmacokinetics. *Curr Top Med Chem* **3:**1257-1268.

Lutz RJ, Dedrick RL and Zaharko DS (1980) Physiological pharmacokinetics: an *in vivo* approach to membrane transport. *Pharmacol Ther* **11:**559-592.

Ma F and Lau CE (1998) Determination of clozapine and its metabolite, N-desmethylclozapine, in serum microsamples by high-performance liquid chromatography and its application to pharmacokinetics in rats. *J Chromatogr B Biomed Sci Appl* **712:**193-198.

Malik AB, Kaplan JE and Saba TM (1976) Reference sample method for cardiac output and regional blood flow determinations in the rat. *J Appl Physiol* **40:**472-475.

Mapleson WW (1973) Circulation-time models of the uptake of inhaled anaesthetics and data for quantifying them. *Br J Anaesth* **1973:**319-334.

Mardia KV, Kent JT and Bibby JM (1979) *Multivariate Analysis.* Academic Press, London.

Nishiyama K, Nishiyama A and Frohlich ED (1976) Regional blood flow in normotensive and spontaneously hypertensive rats. *Am J Physiol* **230:**691-698.

Pitts RF (1974) *Physiology of the Kidney and Body Fluids.* Year Book Medical Publishers, Chicago, ILL.

Poulin P and Theil FP (2000) *A priori* prediction of tissue:plasma partition coefficients of drugs to facilitate the use of physiologically-based pharmacokinetic models in drug discovery. *J Pharm Sci* **89:**16-35.

Rodgers TA (2003) Physicochemical and Structural Determinants of Pharmacokinetic Behaviour, University of Manchester.

Rowland M (1986) Physiologic pharmacokinetic models and interspecies scaling, in *Pharmacokinetics: Theory and Methodology* (Rowland M and Tucker GT eds), pp 69-88, Pergamon Press, Oxford.

Sasaki Y and Wagner HN, Jr. (1971) Measurement of the distribution of cardiac output in unanesthetized rats. *J Appl Physiol* **30:**879-884.

Sugita O, Sawada Y, Sugiyama Y, Iga T and Hanano M (1982) Physiologically based pharmacokinetics of drug-drug interaction: a study of tolbutamide-sulfonamide interaction in rats. *J Pharmacokinet Biopharm* **10:**297 - 316.

Sugiyama Y and Ito K (1998) Future prospects for toxicokinetics: prediction of drug disposition and adverse effects in humans from *in vitro* measurements of drug metabolism, transport and binding. *J Toxicol Sci* **23:**647 - 652.

Taninaka C, Ohtani H, Hanada E, Kotaki H, Sato H and Iga T (2000) Determination of erythromycin, clarithromycin, roxithromycin, and azithromycin in plasma by high-performance liquid chromatography with amperometric detection. *J Chromatogr B Biomed Sci Appl* **738:**405-411.

Teorell T (1937) Kinetics of the distribution of substances administered to the body. I & II. *Arch Int Pharmacodyn* **57:**202-240.

Tsuji A, Yoshikawa T, Nishide K, Minami H, Kimura M, Nakashima E, Terasaki T, Miyamoto E, Nightingale CH and Yamana T (1983) Physiologically based pharmacokinetic model for ß-lactam antibiotics I: tissue distribution and elimination in rats. *J Pharm Sci* **72:**1239 - 1252.

Witten IH and Frank E (2000), in *Data Mining: Practical Machine Learning Tools and Techniques with Java Implementations*, pp 39-41, Morgan Kaufmann Publishers, San Francisco.

Yokogawa K, Ishizaki J, Ohkuma S and Miyamoto K (2002) Influence of lipophilicity and lysosomal accumulation on tissue distribution kinetics of basic drugs: a physiologically based pharmacokinetic model. *Methods Find Exp Clin Pharmacol* **24:**81-93.

Yokogawa K, Nakashima E, Ishizaki J, Maeda H, Nagano T and Ichimura F (1990) Relationships in the structure-tissue distribution of basic drugs in the rabbit. *Pharm Res* **7:**691-696.

Yu L and Amidon G (1999) A compartmental absorption and transit model for estimating oral drug absorption. *Int J Pharm* **186:**119 - 125.

DMD Fast Forward. Published on October 12, 2005 as DOI: 10.1124/dmd.105.004804
This article has not been copyedited and formatted. The final version may differ from this version.

Legends for Figures

FIG. 1. *The 'diffusion-limited' model for tissue distribution, in which the tissue is sub-divided into compartments representing the capillary bed, interstitial fluid and intracellular space.*

Q is the blood flow into and out of the capillary bed; P_vS_v and P_mS_m are the permeability-surface area products for movement across the capillary wall (v) and cell membrane (m), respectively.

FIG. 2. *A simple physiological model for renal clearance, adapted from Katayama et al. (Katayama et al., 1990).*

The subscripted terms are: CB, capillary bed; IF, interstitial fluid; IC, intracellular space. Q_{KI} is the kidney blood flow rate; *GFR* and Q_{UR} are the glomerular filtration rate and urine flow rate, respectively; GFR-Q_{UR} gives the rate of fluid reabsorption that is able to effect compound reabsorption through solvent drag. S represents active secretion of compound, whilst R represents bi-directional movement through passive diffusion.

FIG. 3. *Predicted and observed plasma concentration-time profiles for selected training set compounds: A, clozapine; B, erythromycin; C, pentazocine; D, phenytoin.*

The *in vivo* data (filled symbols) are taken from the literature (Colburn and Gibaldi, 1977; Ichimura et al., 1983; Hanada et al., 1997; Ma and Lau, 1998; Taninaka et al., 2000). The simulated data are the median values (solid line) of a population of predicted profiles generated from 100 stochastic simulations; also indicated are the 10^{th} (dashed line) and 90^{th} (dotted line) percentiles of the population.

FIG. 4. *Predicted and observed plasma concentration-time profiles for selected test set compounds; A, B, C and D correspond to four individual discovery compounds.*

The *in vivo* data (filled symbols) are for proprietary discovery compounds. The simulated data are the median values (solid line) of a population of predicted profiles generated from 100 stochastic simulations; also indicated are the 10^{th} (dashed line) and 90^{th} (dotted line) percentiles of the population.

FIG. 5. *Frequency distribution of the plasma concentration mean fold errors for the training set (A) and test set (B) compounds, and for a reduced test set (C).*

The training set comprises 82 drugs, whilst the test set is composed of 134 discovery compounds; the reduced test set (n = 117) excludes compounds in a particular area of property space for which the accuracy of the PBPK model plasma concentration predictions is likely to be questionable.

FIG. 6. *Descriptive classification model for the expected accuracy of the PBPK model in predicting plasma levels for the test set compounds.*

For the purposes of deriving the illustrated model, a poor plasma concentration prediction was defined as one with mean fold error > 20; all other results were considered satisfactory. According to the model, the criteria $logD < 1.95$ and $fu_p \leq 0.065$ define an area of property space within which the likelihood of obtaining a poor prediction is approximately 60%, represented by 13% of the full test set, but 65% of those compounds for which the plasma concentration predictions were deemed poor.

FIG. 7. *Frequency distribution of the predicted/observed ratios of $AUC_{t1\text{-}tlast\text{-}DN}$ for the training set (A) and test set (B) compounds.*

The training set comprises 82 drugs, whilst the test set is composed of 134 discovery compounds.

FIG. 8. *Frequency distribution of the predicted/observed ratios of $t_{½}$ for the training set (A) and test set (B) compounds.*

The training set comprises 82 drugs, whilst the test set is composed of 134 discovery compounds.

FIG. 9. *Lift chart indicating the success rate of the PBPK model in selecting test set compounds with high* $AUC_{t1\text{-}tlast\text{-}DN}$.

The section criterion was defined as the 25% of the test set compounds with the largest values for $AUC_{t1\text{-}tlast\text{-}DN}$. The dotted line represents the expected success rate if the selections were made at random, the dashed line indicates the maximal success rate and the solid line shows the actual performance of the PBPK model.

FIG. 10. *Principal components scores of transformed values of selected variables for the training set (filled diamonds) and test set (hollow triangles) compounds.*

A, scores for the 1st principal component versus scores for the 2nd principal component; B, scores for the 3rd principal component versus scores for the 2nd principal component. The values for seven selected variables for the training set compounds were transformed by subtracting the mean of the value, and dividing by the standard deviation, so that each transformed variable had a mean of zero and a standard deviation of one. The variable values for the test set were normalized in the same way, using the means and standard deviations of the values for the training set compounds.

Tables

TABLE 1

Summary of the $AUC_{t1\text{-}tlast\text{-}DN}$ and $t_{½}$ predicted/observed ratio distributions for the training set and test set compounds.

	Training Set		Test Set	
Parameter	**Median**	**IQ Range**	**Median**	**IQ Range**
$\boldsymbol{AUC_{t1\text{-}tlast\text{-}DN}}$	0.83	0.44-1.46	0.67	0.36-1.39
$\boldsymbol{t_{½}}$	1.02	0.65-1.66	1.75	0.92-4.05

DMD Fast Forward. Published on October 12, 2005 as DOI: 10.1124/dmd.105.004804
This article has not been copyedited and formatted. The final version may differ from this version.

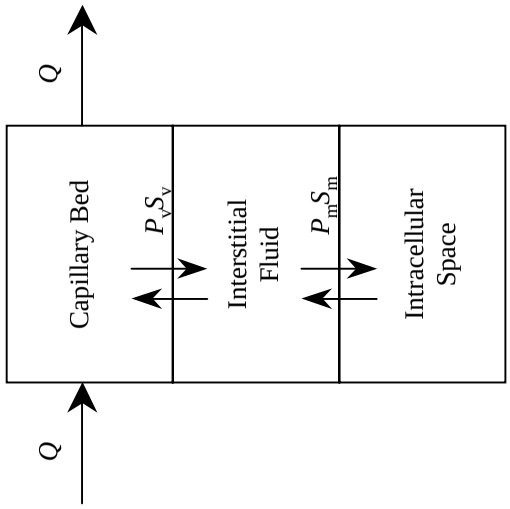

FIG. 1.

DMD Fast Forward. Published on October 12, 2005 as DOI: 10.1124/dmd.105.004804
This article has not been copyedited and formatted. The final version may differ from this version.

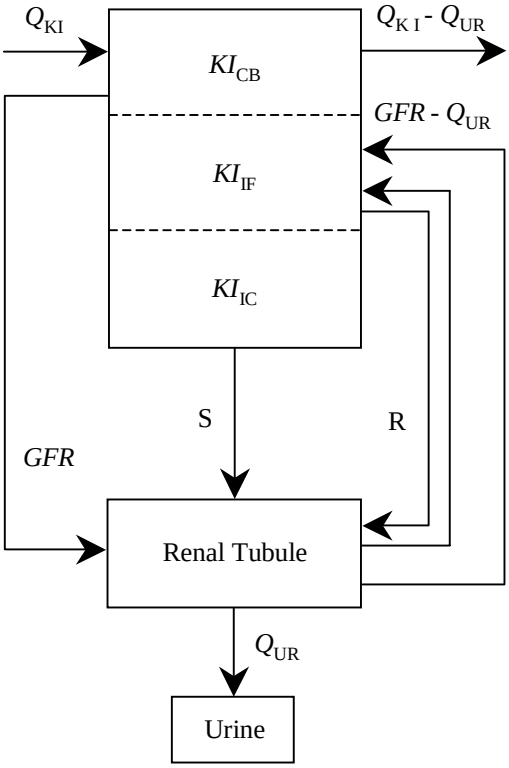

FIG. 2.

DMD Fast Forward. Published on October 12, 2005 as DOI: 10.1124/dmd.105.004804
This article has not been copyedited and formatted. The final version may differ from this version.

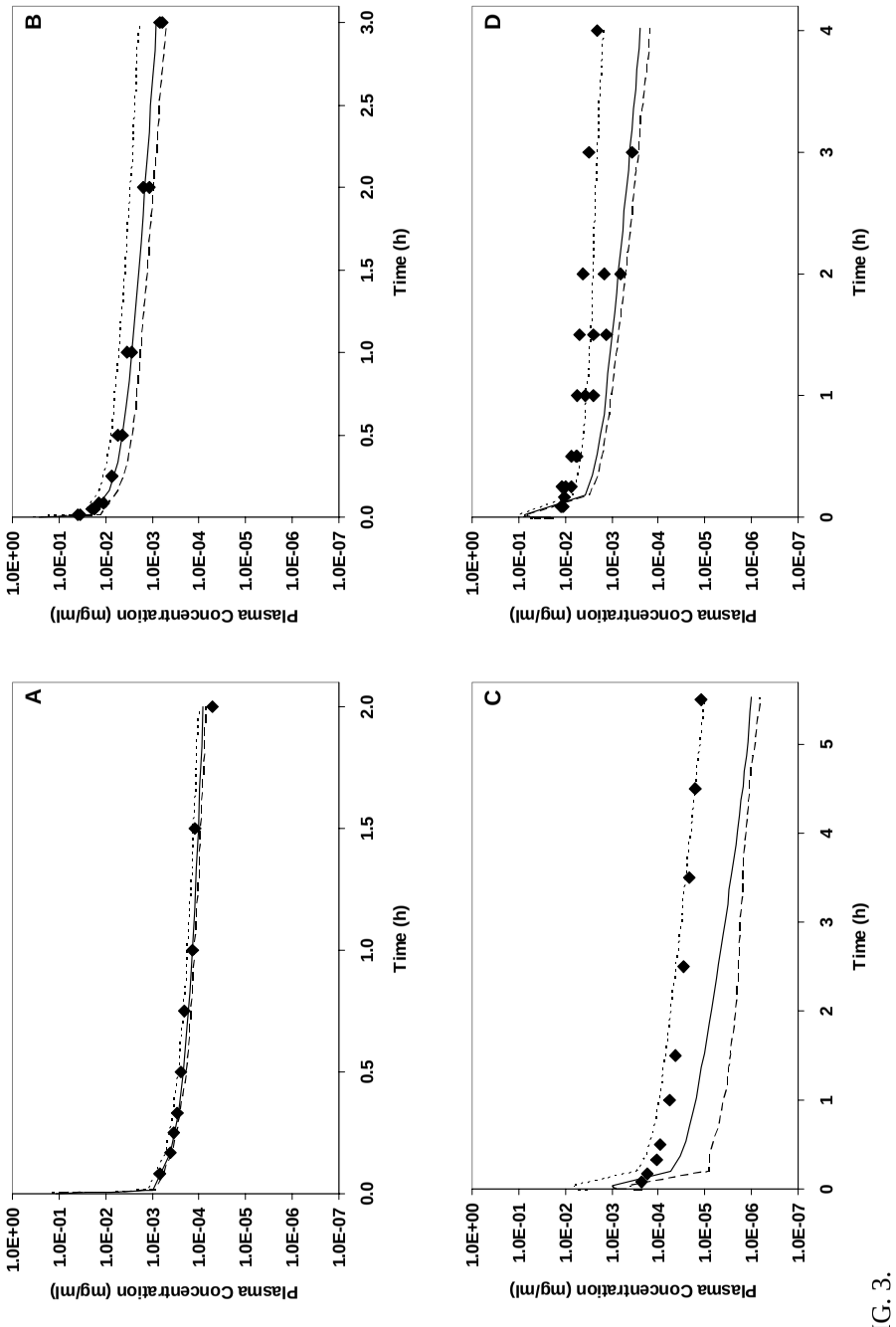

FIG. 3.

DMD Fast Forward. Published on October 12, 2005 as DOI: 10.1124/dmd.105.004804

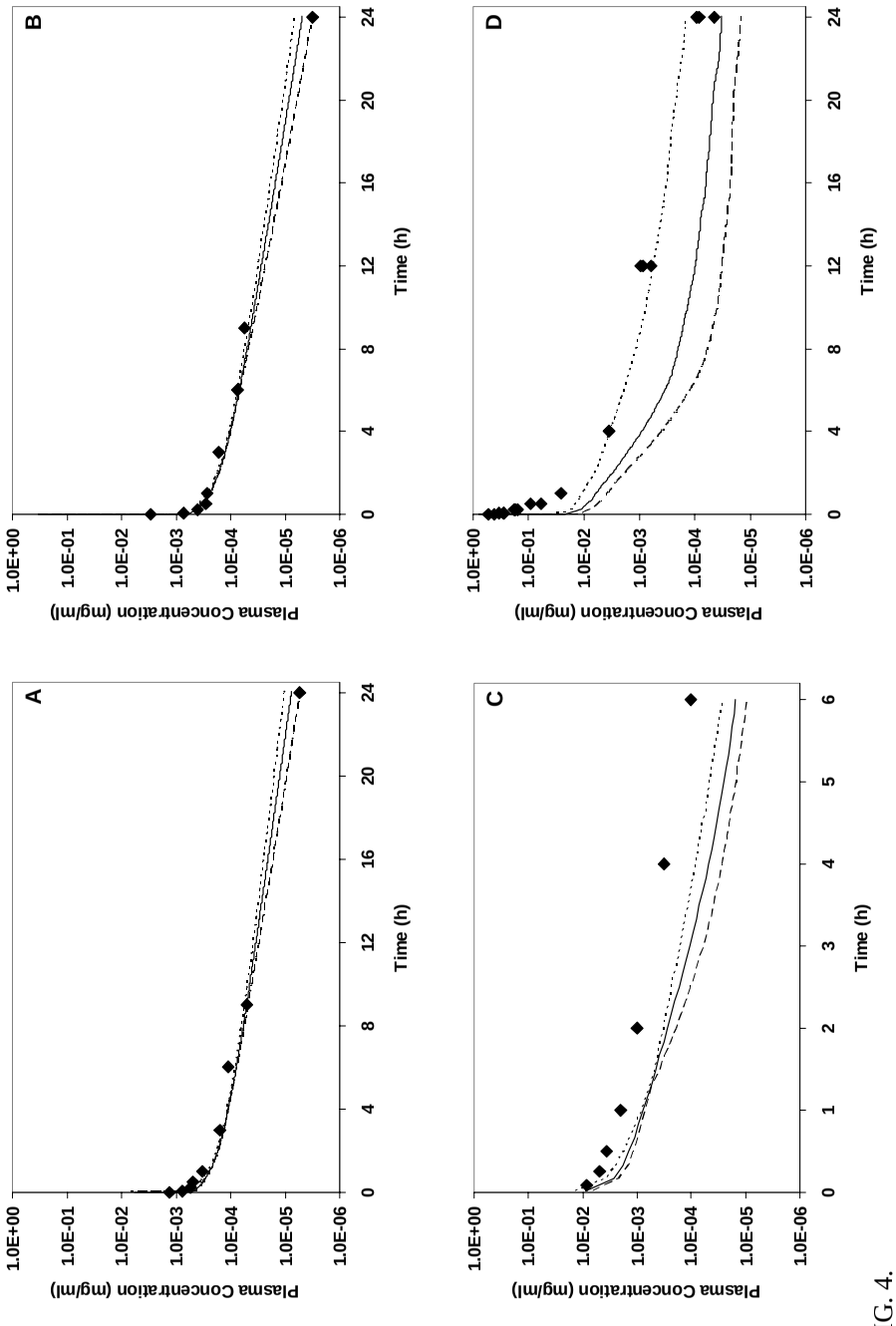

FIG. 4.

DMD Fast Forward. Published on October 12, 2005 as DOI: 10.1124/dmd.105.004804
This article has not been copyedited and formatted. The final version may differ from this version.

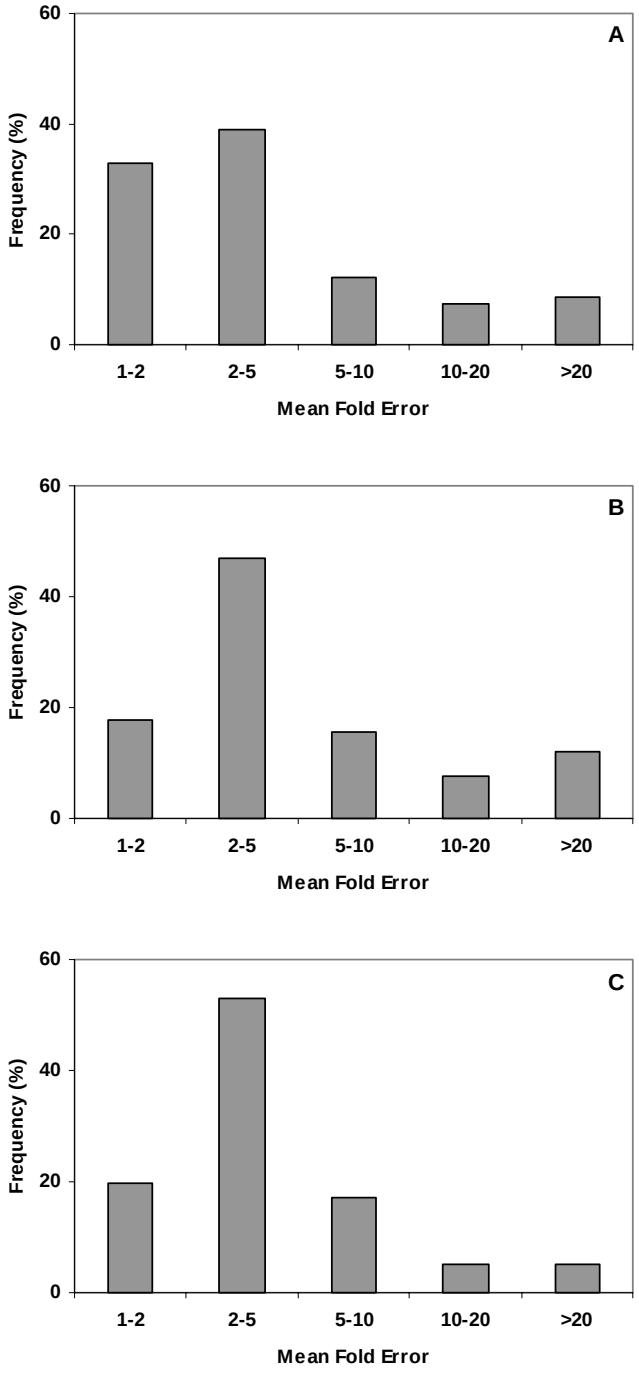

FIG. 5.

DMD Fast Forward. Published on October 12, 2005 as DOI: 10.1124/dmd.105.004804
This article has not been copyedited and formatted. The final version may differ from this version.

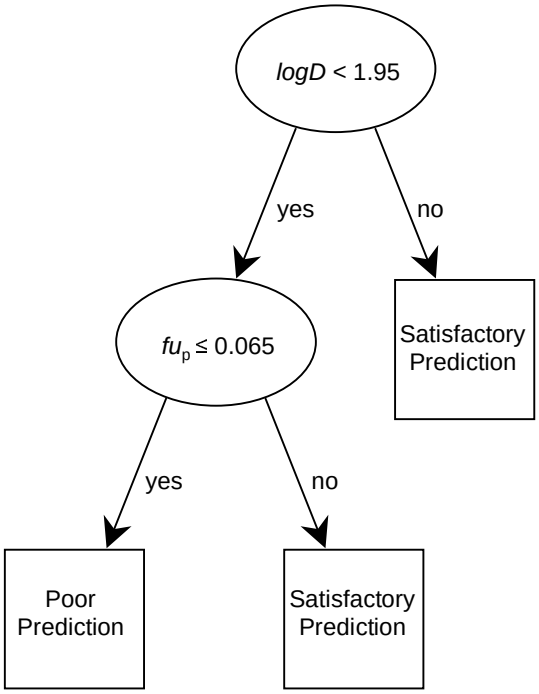

FIG. 6.

DMD Fast Forward. Published on October 12, 2005 as DOI: 10.1124/dmd.105.004804
This article has not been copyedited and formatted. The final version may differ from this version.

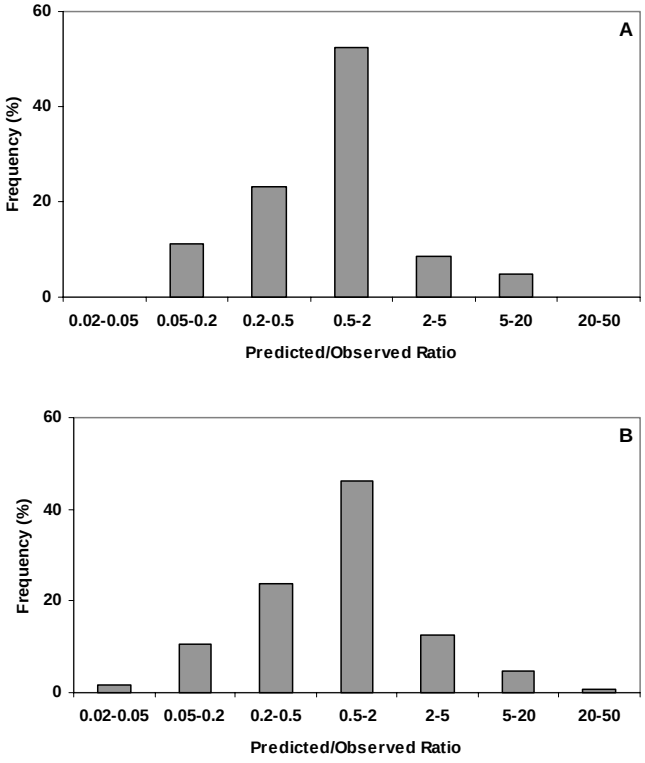

FIG. 7.

DMD Fast Forward. Published on October 12, 2005 as DOI: 10.1124/dmd.105.004804
This article has not been copyedited and formatted. The final version may differ from this version.

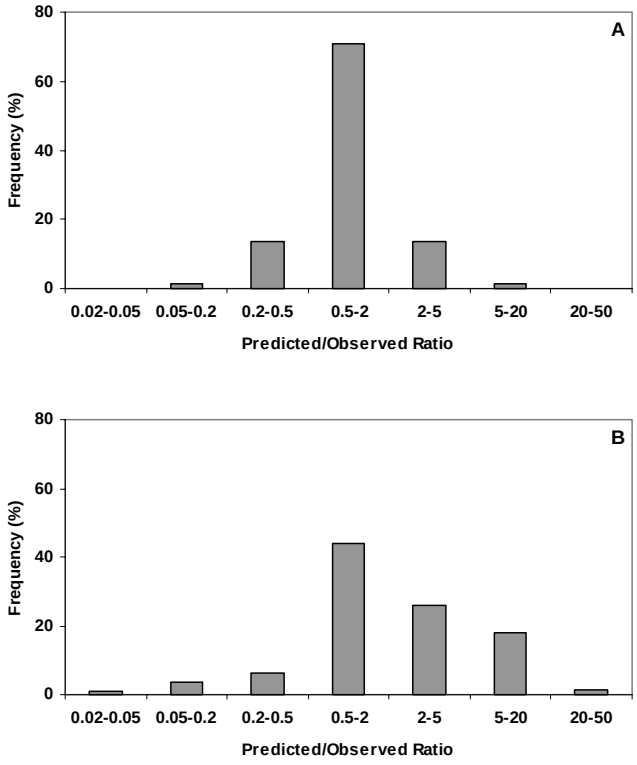

FIG. 8.

DMD Fast Forward. Published on October 12, 2005 as DOI: 10.1124/dmd.105.004804
This article has not been copyedited and formatted. The final version may differ from this version.

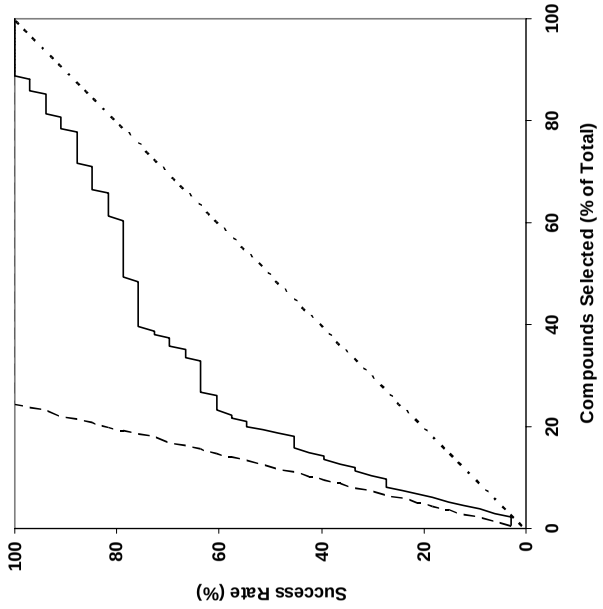

FIG. 9.

DMD Fast Forward. Published on October 12, 2005 as DOI: 10.1124/dmd.105.004804
This article has not been copyedited and formatted. The final version may differ from this version.

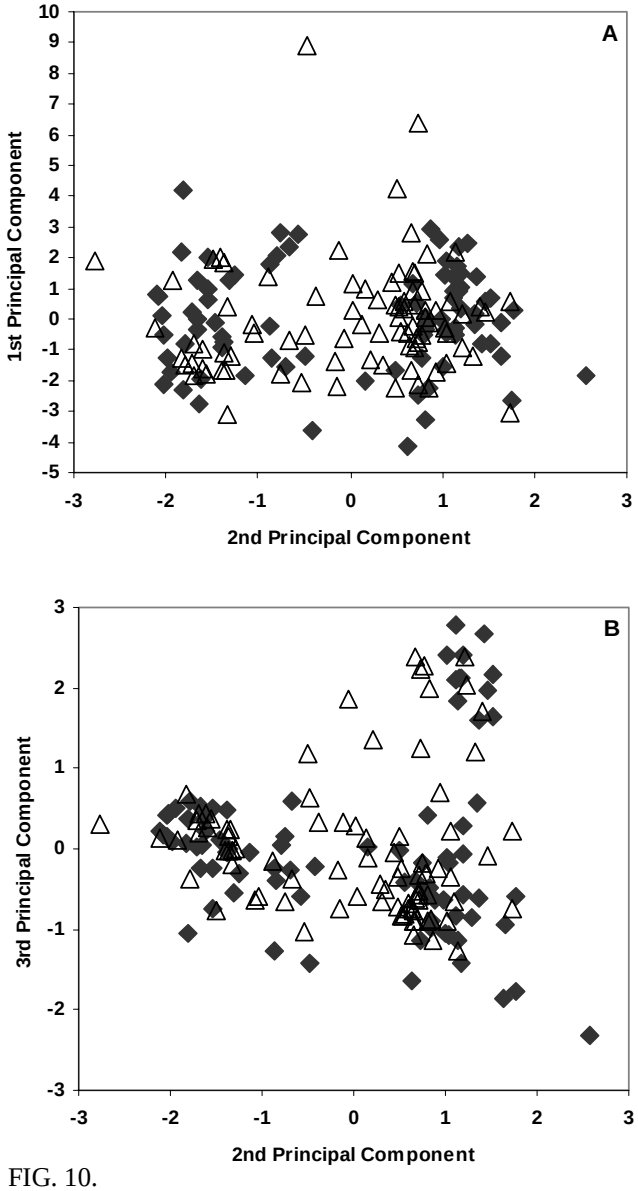

FIG. 10.